

# UV Autofluorescence Microscopy of Oklahoma Permian Synapsid Femur (*Dimetrodon* Cope, 1878) Reveals Blood Clots in Vascular Canals

Mark H. Armitage

DSTRI, Inc. 325 East Washington St., #170, Sequim, WA 98382

micromark@juno.com

**Abstract:** *Dimetrodon* sp. femur, jaw, teeth, and rib bones were collected at N.E. Frederick, OK, and sectioned for histological examination. This Oklahoma Museum of Natural History site has yielded well-preserved Paleozoic fossils for decades. All bones were heavily infiltrated with calcite and other minerals, yet a reddish-brown mass obstructed many vascular channels. This reddish-brown mass reacted to 374 nm UV illumination by emitting bright blue autofluorescence. This was true for every specimen and indicates a heavy presence of iron. We conclude that the iron in the canals is the crystallized remains of blood that clotted during an asphyxiation event that killed the animal. Remarkably similar reddish-brown obstructive material has also been observed in other histological studies performed on *Dimetrodon* bones. We conclude that these are also the remains of blood clots and simply await examination under UV fluorescence.

**Keywords:** *Dimetrodon*, blood clots, autofluorescence, femur, vasculature

## Introduction

The Lower Permian N.E. Frederick fossil site (Sam Noble Oklahoma Museum of Natural History V 173, Tillman County, OK), which is located 47 miles from Richards Spur, OK, yielded permineralized synapsid femur, jaw, tooth, and rib specimens (Paleozoic) in May of 2021 (Figures 1–5) that were subjected to a petrographic study. Site V 173 is noted for yielding exceptional Lower Permian bones from fish, sharks, amphibians, and reptiles from over 28 genera, including *Dimetrodon* [1–5].

Skeletal remains of Paleozoic terrestrial animals have been recovered from Illinois [6], Utah [7], and Europe [8], however, the best sites are in Oklahoma [5] and Texas [9–17]. Synapsid specimens such as *Dimetrodon* are rare worldwide, but of Oklahoma it has been said, “tens of thousands of [Paleozoic] collected specimens” are preserved from one site alone, Richards Spur [3]. *Dimetrodon*, the subject of this study, has been collected widely across North America [1,6,7,9–15] with most of the 12 known species of *Dimetrodon* coming from Texas [16–20].

Few histological reports of *Dimetrodon* or other synapsid bones exist, but teeth, long bones, and vertebra have been sectioned and reported [16–20]. Those reports are compared to the material presented here: *Dimetrodon* femur (DSTRI-5-4-G, Figures 1–2), jaw (DSTRI-5-4-Ja, Figure 3), tooth (DSTRI-5-4-Jb, Figure 4, red arrow), and rib (DSTRI-5-4-K, Figure 5). The purpose of this study was to examine ground sections of *Dimetrodon* bone for evidence of blood clots in vessel canals.

## Materials and Methods

*Dimetrodon* specimens were collected from pebbly and granular surface deposits on a lower Permian bed near the shoreline of Lake Frederick, OK. Bones were placed into 10% formalin for transport to the lab. A newly sanitized laboratory

space was secured and entry restricted to only two technicians. Bones were rinsed in distilled water, air-dried, and specimen ID numbers painted on the reverse. After stabilizing at room temperature for 5 days, ground sections approximately 40 microns thick were coated with a liquid polymer for stability and cured overnight, but not coverslipped. Sections, without coverslips, were viewed with 374 nm UV autofluorescence microscopy for evidence of blood clots in vascular canals, as described by Armitage and Solliday [21].

## Results

The *Dimetrodon* femur (DSTRI-5-4-G, Figures 1–2) was approximately 11 cm long and 3 cm wide at mid-diaphysis when located *in situ*. Severe dorsoventral crushing of the femur must have occurred at death or during burial because multiple 2 to 3 mm wide fractures were preserved through permineralization. Under brightfield examination, reddish-brown opaque masses filled the entire lumen of many vascular canals (Figure 6a). When subjected to UV autofluorescence, the masses fluoresced brightly, as observed previously with ground sections of Cretaceous bone [21] (Figure 6b, de-colored). More femur-filled vascular canals with glowing masses are seen in Figures 7 and 8. We interpret these masses to be clotted blood, which remained *in situ*, filling the vessel canals [21].

Jaw (DSTRI-5-4-Ja, Figures 9a, 9b), tooth (DSTRI-5-4-Jb, Figures 10a, 10b, and 11a, 11b) and rib (DSTRI-5-4-K, Figures 12a, 12b and 13, 14) ground sections likewise exhibited clots, which filled the lumens of most vascular canals and glowed brightly under UV autofluorescence. Straight-line polishing marks are clearly seen across the areas where iron was exposed and polished (Figures 8a, 8b, 11a, 11b, 12b, 13, 14), typical of a malleable metal. Polishing marks are only visible under reflected light (fluorescence, brightfield, or darkfield). A steel pin extended over the field diaphragm of the microscope (Figure 15) demonstrates that the iron in the clot is more dense than the steel pin visible underneath the clotted canal. All bones were deeply infiltrated with calcite, (yellow color in polarized light with a compensator), yet clots remained as clogs in many canals (Figure 16, green arrows). Remaining *Dimetrodon* material from this study is reposited at DSTRI, Inc., Mansfield, TX.

## Discussion and Conclusions

The surface of site V 173 was littered with varying sizes of pebbles, stones, and bone fragments, ranging from dark to bone-white in color. These shards and pebbles were found touching and surrounding the collected bones (Figure 1). Bones and fragments came away from the surface only with some tugging, as if they were cemented in place. The color of



Figure 1: *Dimetrodon* femur, in situ, N.E. Frederick, OK.

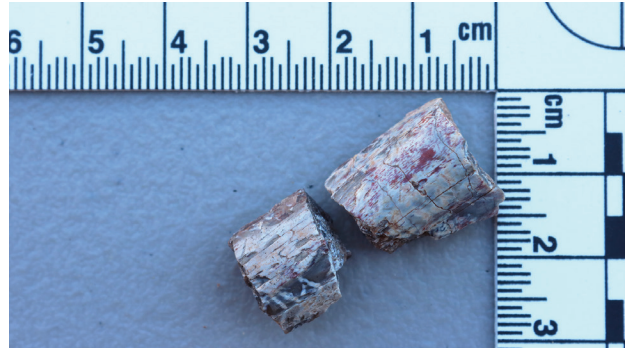


Figure 5: Portion of *Dimetrodon* rib sent for sectioning.



Figure 2: Portion of *Dimetrodon* femur sent for sectioning.

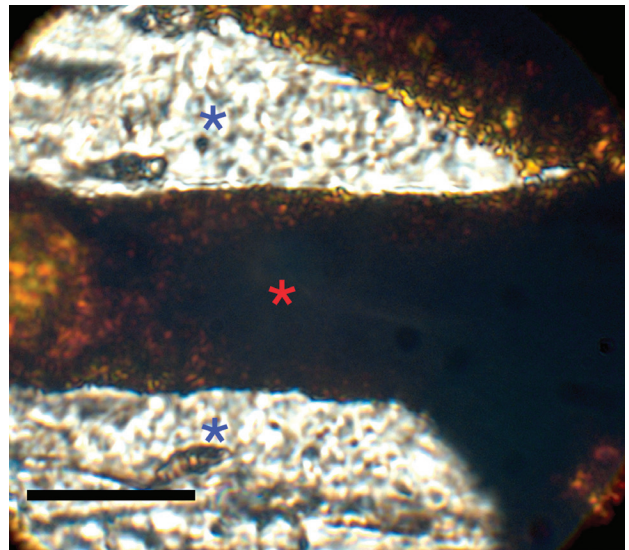


Figure 6a: Brightfield image of clot in femur vascular canal (red asterisk) and infiltrated calcite (blue asterisks). Note granular nature of clot. Scale bar=100µm.



Figure 3: Portion of *Dimetrodon* jaw sent for sectioning.



Figure 4: Portion of *Dimetrodon* tooth sent for sectioning.

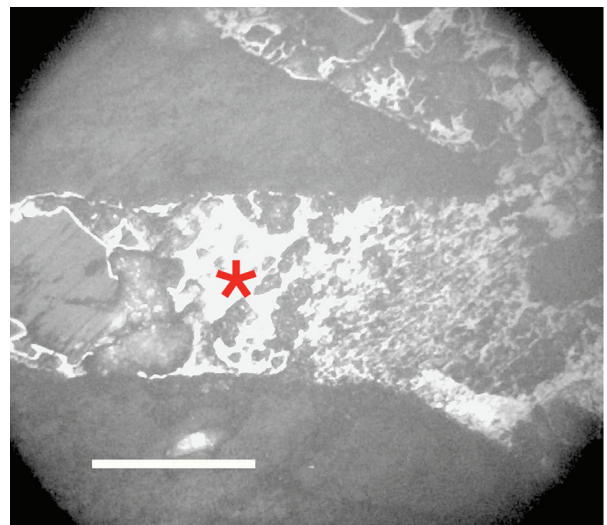
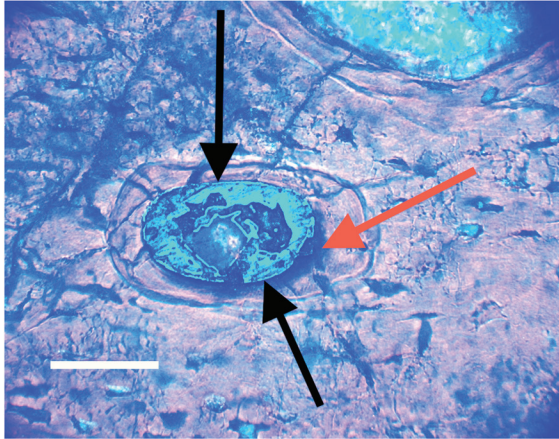
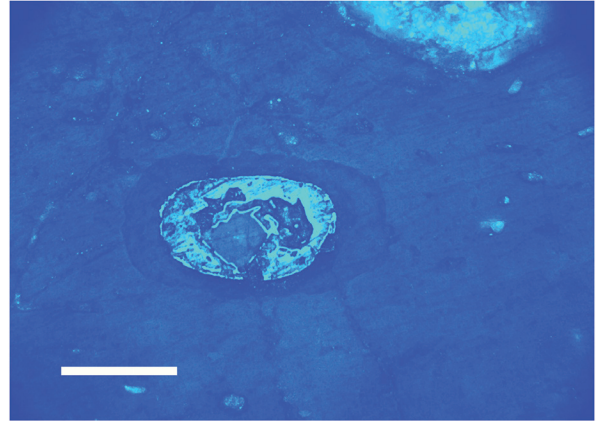


Figure 6b: Ultraviolet fluorescence image of clot from Figure 6a (de-colored). Note bright, uniform autofluorescence signal from iron in clot (red asterisk). Crystallized blood products are the dark inclusions within the clot. Scale bar=100µm.



**Figure 7a:** Ultraviolet fluorescence and brightfield combined image of Haversian canal with femur clot blocking the entire lumen. A bright line of demarcation at the outer edges of the clot (black arrows) shows that the iron did not escape the canal. Deeper portion of the clot extending downward into the canal (red arrow). Scale bar=80µm.



**Figure 7b:** Ultraviolet fluorescence image of the clot from 7a. Scale bar=80µm.

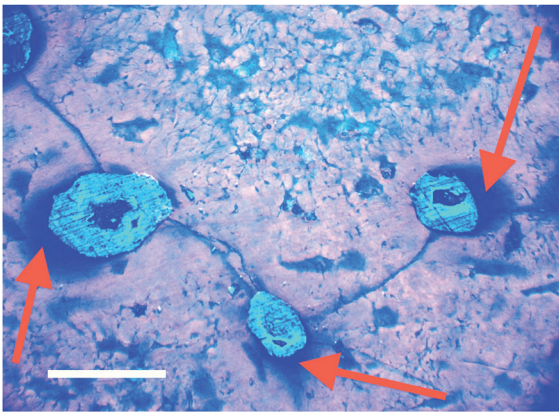


**Figure 8a:** Several clots from *Dimetrodon* femur. Orange arrows indicate the lumen-filling clot extending deeper into the vascular canal below the plane of focus. Note the polishing marks in the malleable metal clot. Scale bar=60µm.

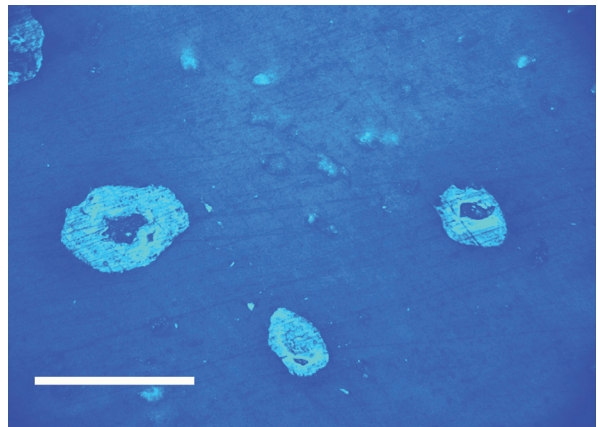


**Figure 8b:** Ultraviolet fluorescence image of the clots from 8a. Scale bar=60µm.

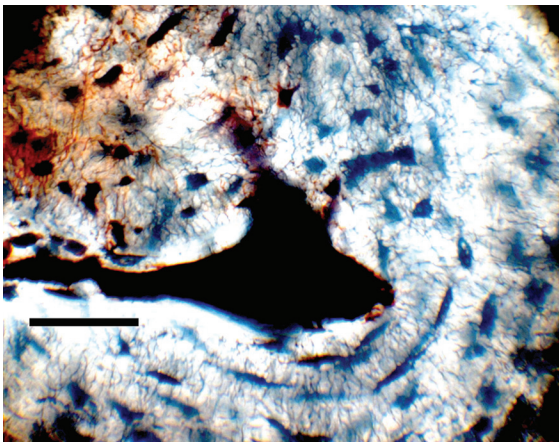


**Figure 9a:** Brightfield image, *Dimetrodon* jaw. Blood clot filling a Haversian vessel canal. Scale bar=60µm.

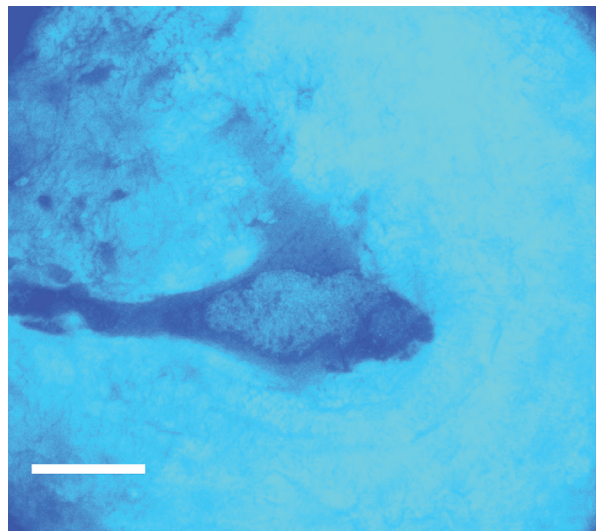


**Figure 9b:** Ultraviolet image of the clot from 9a. Scale bar=60µm.

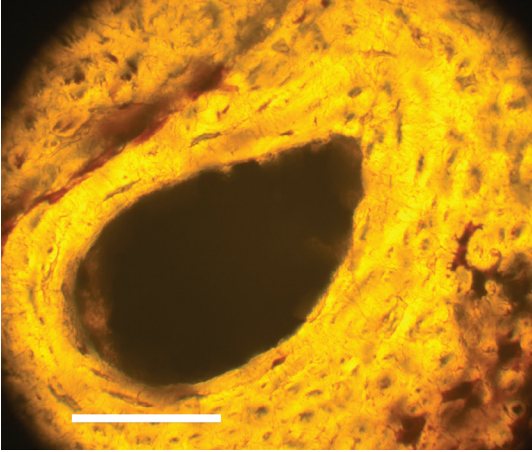


**Figure 10a:** Brightfield image, *Dimetrodon* tooth, clot filling a Haversian vessel canal. Scale bar=60  $\mu$ m.

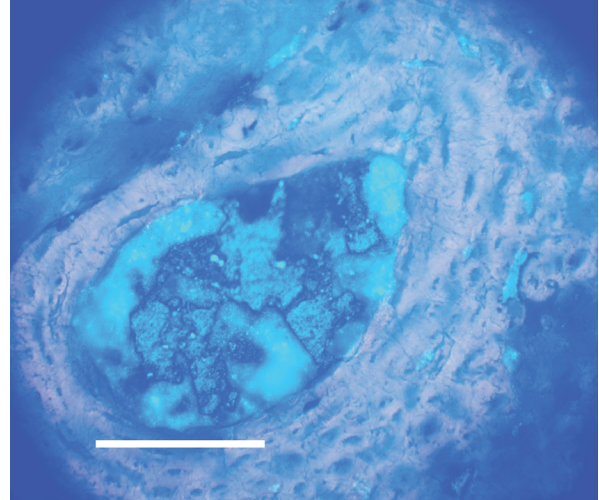


**Figure 10b:** Ultraviolet image of the clot from 10a. Scale bar=60  $\mu$ m.

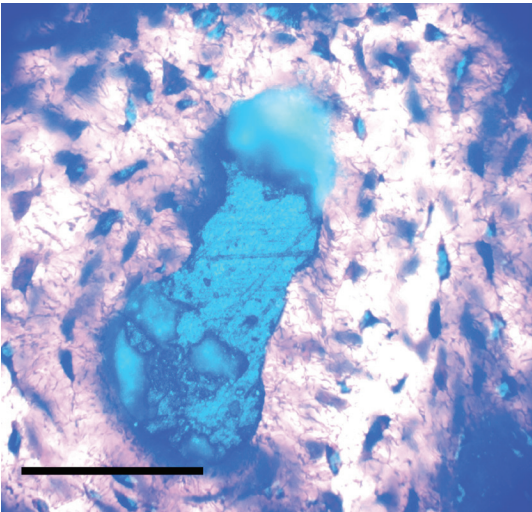


**Figure 11a:** Combined brightfield and ultraviolet fluorescence image, *Dimetrodon* tooth, clot filling a Haversian vessel canal. Note polishing marks on iron, indicating it is malleable. Scale bar=60  $\mu$ m.

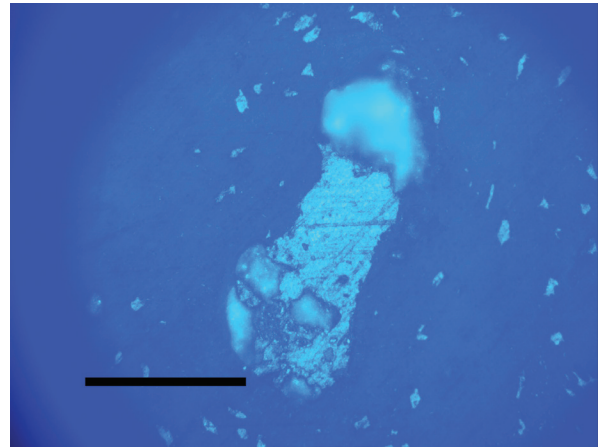


**Figure 11b:** Ultraviolet fluorescence image of the clot from 11a. Scale bar=60  $\mu$ m.

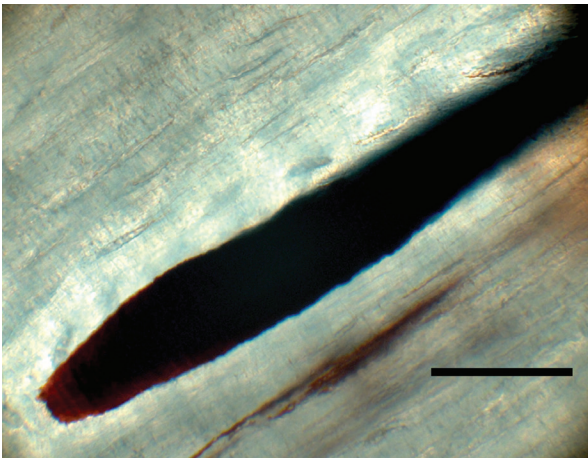


**Figure 12a:** Brightfield image, *Dimetrodon* rib, clot filling a Haversian vessel canal. Scale bar=60  $\mu$ m.

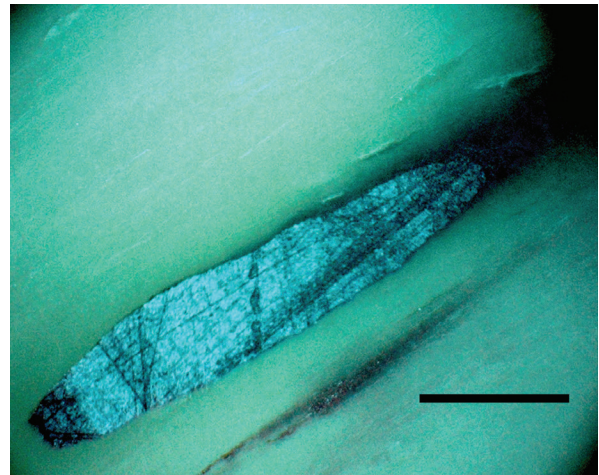


**Figure 12b:** Ultraviolet fluorescence image of the clot from 12a. Note polishing marks on iron, indicating it is malleable. Scale bar=60  $\mu$ m.

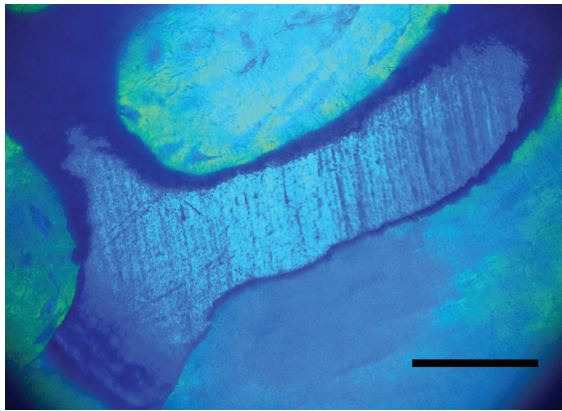


**Figure 13:** Ultraviolet fluorescence image, *Dimetrodon* rib. Clot filling right side of bifurcated canal. Note polishing marks on iron, indicating it is malleable. Scale bar = 60  $\mu$ m.

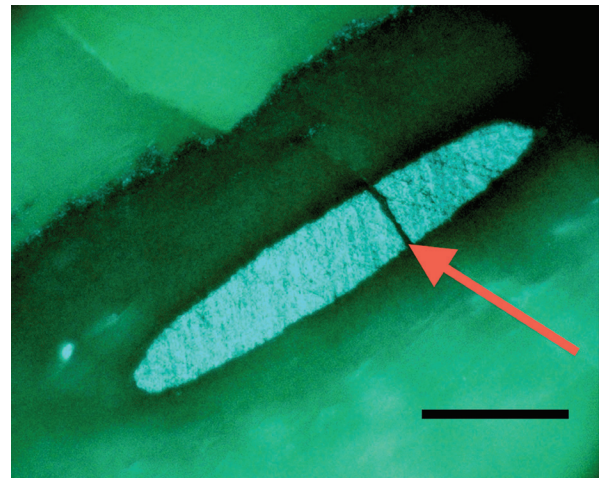


**Figure 14:** Ultraviolet fluorescence image, *Dimetrodon* rib. Clot filling Haversian canal. Note polishing marks and that the crack through the bone cleanly split the iron clot. Scale bar = 60  $\mu$ m.

the subsurface material, a non-calcareous, silty clay, was darker than the bleached lighter color of the surface and contained significant moisture due to severe thunderstorms that had been active in the area just a week before collection began.

We compared our brightfield observations of reddish-brown clots in *Dimetrodon* specimens with histology studies of other Paleozoic bones. Shelton et al. [17] transversely sectioned *D. natalis* femora as well as humeri collected from Texas. Cross-section images of those bones showed infiltration of calcite and other minerals, and significant dark and opaque masses remained within each medullary cavity. Brink and Reisz also sectioned *D. grandis* teeth from Texas [18]. We conclude that the dark areas seen on Figure 5D of that work are probably clots. Huttenlocker and Shelton transversally sectioned *Dimetrodon* sp. humeri from Oklahoma [19]. Although we produced longitudinal sections in *Dimetrodon*, there is remarkable similarity between our Figure 16 and Figures 3, 5, and 6 of that study. Canals in both studies exhibit the same reddish-brown clots at the center of Haversian systems. Agliano et al. [20] sectioned *Dimetrodon* vertebrae and showed deeply clotted canals in their Figures 4 and 5. All of these ground specimens need examination under UV-autofluorescence to confirm our findings. Finally, we note the well-known work by Davis on vertebrate bones from the lower Permian [22]. We counted 45 images of sections of Paleozoic material in that work, which includes *Dimetrodon*, and many of the images show robust clots. We would especially draw attention to the plates on pages 354–57 as a particularly good example of clots within *Dimetrodon* teeth and vertebrae.

A discussion of disseminated intravascular coagulation (DIC), which is a clotting condition typical of drowning victims, exceeds the purpose of this paper, as it was detailed in a previous work [21]. These results show that *Dimetrodon* bones collected in the Lower Permian of Oklahoma display heavy clotting within vascular canals suggesting that DIC was the cause of death, followed by burial and mineral replacement that did not dislodge all clots from vessel canals.

### Acknowledgements

Thanks to Bill and Julie May from the Sam Noble Oklahoma Museum of Natural History for site guidance, collection, and identification assistance and for constructive

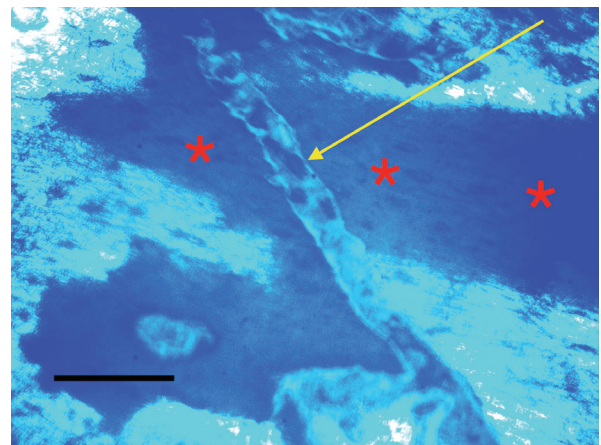


**Figure 15:** Ultraviolet fluorescence image, *Dimetrodon* jaw. Note the steel pin, mounted over the field diaphragm (red asterisks) indicating the thin clot (yellow arrow) is denser than the pin. Scale bar = 60  $\mu$ m.

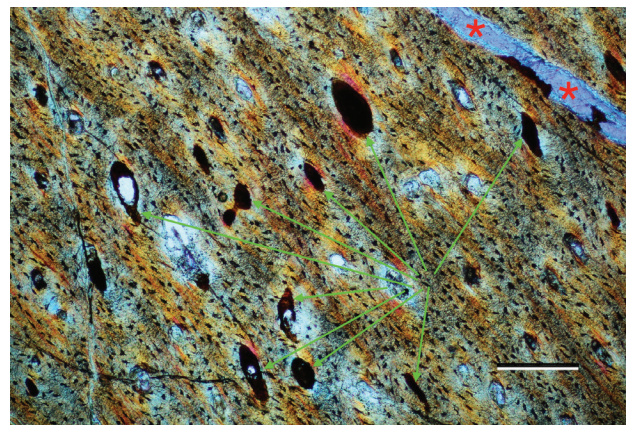


**Figure 16:** Crossed polarized image of *Dimetrodon* femur. Note infiltrating calcite (red asterisks) and the many clotted canals (green arrows). Scale bar = 275  $\mu$ m.

comments. Thanks also to Joe Taylor and Stan Lutz from the Mt. Blanco Fossil Museum, and DSTRI, Inc. personnel for assistance and funding.

## References

- [1] ED Cope, *Trans Amer Phil Soc* 16 (1888) <https://doi.org/10.2307/1005392>.
- [2] J Zidek et al., *Oklahoma Geol Notes* 63 (2003) 136–47 <http://ogs.ou.edu/docs/geologynotes/GN-V63N4.pdf>.
- [3] DC Evans et al., *Paleontology* 52 (2008) <https://doi.org/10.1111/j.1475-4983.2008.00837.x>.
- [4] J Woodhead et al., *Geology* 38 (2010) <https://doi.org/10.1130/G30354.1>.
- [5] MJ MacDougall et al., *Palaeogeog Palaeoclimatol Palaeoecol* 475 (2017) <https://doi.org/10.1016/j.palaeo.2017.02.019>.
- [6] ED Cope, *Proc Acad Nat Sci Phila* (1875) <https://www.jstor.org/stable/4624504>.
- [7] PP Vaughn, *NM Geol Soc 24th Field Conf Guide* (1973) HL James, ed. pp 99–105 [https://nmgs.nmt.edu/publications/guidebooks/downloads/24/24\\_p0099\\_p0105.pdf](https://nmgs.nmt.edu/publications/guidebooks/downloads/24/24_p0099_p0105.pdf).
- [8] DS Berman et al., *Canadian J Earth Sci* 38 (2001) <https://doi.org/10.1139/cjes-38-5-803>.
- [9] ED Cope, *Proc Amer Phil Soc* 17 (1877) <https://jstor.org/stable/982295>.
- [10] ED Cope, *Proc Amer Phil Soc* 17 (1878) <https://jstor.org/stable/982652>.
- [11] ED Cope, *Proc Amer Phil Soc* 19 (1880) <https://jstor.org/stable/982605>.
- [12] AS Romer, *J Geol* 35 (1927) <https://jstor.org/stable/30060393>.
- [13] EC Olson, *Evolution* 6 (1951) <https://doi.org/10.1111/j.1558-5646.1952.tb01413.x>.
- [14] KW Craddock and RW Hook, *49th Ann Mtg Soc Vertebrate Paleontol Field Trip Guidebook Number 2* (1989) pp 40–46 [https://www.researchgate.net/profile/Robert-Hook-2/publication/350850396\\_An\\_overview\\_of\\_vertebrate\\_collecting\\_in\\_the\\_Permin\\_System\\_of\\_North-Central\\_Texas/links/60760f4392851cb4a9dc0ff3/An-overview-of-vertebrate-collecting-in-the-Permian-System-of-North-Central-Texas.pdf](https://www.researchgate.net/profile/Robert-Hook-2/publication/350850396_An_overview_of_vertebrate_collecting_in_the_Permin_System_of_North-Central_Texas/links/60760f4392851cb4a9dc0ff3/An-overview-of-vertebrate-collecting-in-the-Permian-System-of-North-Central-Texas.pdf).
- [15] GA Florides et al., *J Thermal Biol* 26 (2001) [https://doi.org/10.1016/S0306-4565\(00\)00019-X](https://doi.org/10.1016/S0306-4565(00)00019-X).
- [16] AK Huttenlocker et al., *J Morphol* 271 (2010) <https://doi.org/10.1002/jmor.10876>.
- [17] CD Shelton et al., *Earth Env Sci Trans Royal Soc Edinburgh* 103 (2013) 217–36 <https://doi.org/10.1017/S175569101300025X>.
- [18] KS Brink and RR Reisz, *Nat Commun* 5 (2013) <https://doi.org/10.1038/ncomms4269>.
- [19] AK Huttenlocker and CD Shelton, *Phil Transact Royal Soc B* 375 (2020) <https://doi.org/10.1098/rstb.2019.0142>.
- [20] A Agliano et al., *Anat Rec* 304 (2020) <https://doi.org/10.1002/ar.24468>.
- [21] MH Armitage and J Solliday, *Microscopy Today* 28 (2020) <https://doi.org/10.1017/S1551929520001340>.
- [22] *The Lower Permian Vertebrates of Waurika, Oklahoma, volume 1* (2018) K Davis, ed., NHBS, UK. <https://www.nhbs.com/the-lower-permian-vertebrates-of-waurika-oklahoma-book>.

MT

# Don't Let a Fingerprint Ruin Your Day—Use Evactron® Cleaning



Fingerprints are one of the major sources of contamination in vacuum systems. Evactron dual-action *turbo plasma cleaning™* expels these adventitious hydrocarbons with:

- ❖ Oxygen radicals plus UV active desorption
- ❖ Hollow cathode plasma radical source
- ❖ No kinetic sputter etch damage or debris
- ❖ A compact and efficient plasma source
- ❖ Cleaning in minutes for days of perfect imaging and analysis



**Need clean samples and chamber surfaces?  
Let us show you the  
“fastest way to pristine”™!**

**WWW.EVACTRON.COM 1-650-369-0133**